Original Article *Bulletin of Pure and Applied Sciences.*
Vol. 38E (Math & Stat.), No.1, 2019. P.193-207
Available online at www.bpasjournals.com
Print version ISSN 0970 6577
Online version ISSN 2320 3226
DOI: 10.5958/2320-3226.2019.00017.1

BUOYANCY EFFECTS ON CHEMICALLY REACTIVE MAGNETO-NANOFLUID PAST A MOVING VERTICAL PLATE

P. Chandra Reddy[1*], K. Venkateswara Raju[2], M. Umamaheswar[1], M. C. Raju[3]

Author Affiliation:
[1]Department of Mathematics, Annamacharya Institute of Technology and Sciences (Autonomous), Rajampet, Andhra Pradesh 516126, India.
[2]Department of Basic Sciences & Humanities, Sree Vidyanikethan Engineering College (Autonomous), A. Rangampet, Tirupati, Andhra Pradesh 517102, India.
[3]Department of Mathematics, JNTUA College of Engineering, Pulivendula, Andhra Pradesh 516390, India.

***Corresponding Author:**
P. Chandra Reddy, Department of Mathematics, Annamacharya Institute of Technology and Sciences (Autonomous), Rajampet, Andhra Pradesh 516126, India.
E mail: chandramsc01@gmail.com

Received on 15.08.2018 Revised on 28.02.2019 Accepted on 07.04.2019

Abstract: The present work is a study on free convective heat and mass transfer characteristics of chemically reactive magneto-nanofluid flow through a vertical moving porous plate in conducting field. A water-based nanofluid with the combination of alumina is considered in this analysis. The governing equations of motion are solved by applying the finite difference method. The influence of different parameters on fluid velocity, temperature, concentration, shear stress, rate of heat transfer and rate of mass transfer are presented graphically and discussed. The novelty of this study is the consideration of occurrence of chemical reaction. The influence of chemical reaction leads to an enhancement in the concentration of the fluid and a diminution in its temperature.

Keywords: Free convection, Magneto-nanofluid, Heat generation, Moving vertical porous plate, Conducting field and Chemical reaction.

2010 AMS Mathematics Subject Classification: 76M20, 76S05, 76S99, 76V05, 76V99, 76W05, 76W99, 80A32, 80M20.

1. INTRODUCTION

Nanofluids are formed by mixing different nano particles into base fluid. Such fluids play a significant role in the industries and chemical factories because of their unique physical and chemical properties. These fluids are more utilized by the industrialists based on their high thermal conductivity when compared to other fluids. Magnetohydrodynamic (MHD) flow with heat and mass transfer has essential applications for real world problems in physics, chemistry and engineering. MHD boundary layers are considered and implemented effectively in various technical fields employing liquid metals and also plasma flow of magnetic fields. In the recent years many researchers have contributed in studying the influences of electrically conducting nanofluids in the presence of a magnetic field on the flow and heat transfer of an incompressible viscous fluid. A review of convective heat transfer enhancement with nanofluids was given by Kakac and Pramuanjaroenkij [1]. Turkyilmazoglu [2] presented exact analytical solutions for heat and mass transfer effects on magnetohydrodynamic slip flow in nanofluids. Srinivasacharya and Srinivasacharya and Upendar [3] analyzed free convection in MHD micropolar fluid with Soret and Dufour effects. Raju et al. [4] investigated Soret effects due to natural convection between heated inclined plates with magnetic field. Chandra Reddy et al. [5] examined thermal and solutal buoyancy effect on MHD boundary layer flow of a visco-elastic fluid past a porous plate with varying suction and heat source in the presence of thermal diffusion. Makinde and Aziz [6] considered MHD mixed convection past a vertical plate embedded in a porous medium with a convective boundary condition. Kandasamy et al. [7] examined and reported the effects of chemical reaction, heat and mass transfer on boundary layer flow through a porous wedge with heat radiation in the existence of suction or injection. Hayat et al. [8] analyzed slip and Joule heating effects on mixed convection peristaltic transport of nanofluid with Soret and Dufour effects. Chandra Reddy et al. [9] analyzed magnetohydrodynamic convective double diffusive laminar boundary layer flow past an accelerated vertical plate. Further Chandra Reddy et al. [10, 11] studied free convective heat and mass transfer flow of heat generating nano fluid past a vertical moving porous plate in conducting field. Chand and Rana [12] studied magneto convection in a layer of nanofluid through porous medium with more realistic approach. Anjali Devi and Mekala Selvaraj [13] examined and reported thermal radiation effects of hydromagnetic flow of nanofluid over a nonlinear stretched sheet in the presence of variable heat generation and viscous dissipation. Murthy et al. [14] analyzed and reported the significance of viscous dissipation and chemical reaction on convective transport in a boundary layer stagnation point flow through a stretching or shrinking sheet in a nanofluid. Motsumi and Makinde [16] examined the effects of thermal radiation and viscous dissipation on boundary layer flow of nanofluids over a permeable moving flat plate. Kameswaran et al [17] considered and analyzed hydro-magnetic nanofluid flow due to a stretching or shrinking sheet with viscous dissipation and chemical reaction effects. Nield and Kuznetsov [18] discussed the Cheng–Minkowycz problem for the double-diffusive natural convective boundary layer flow in a porous medium saturated by a nanofluid. Ahmad et al [19] gave solutions for Blasius and Sakiadis problems in nanofluids. Abolbashari et al. [20] reported entropy analysis for an unsteady MHD flow past a stretching permeable surface in nano-fluid. Sheikholeslami and Rashidi [21] examined the effect of space dependent magnetic field on free convection of Fe_3O_4-water nanofluid. Rashidi et al. [22] derived Lie group solution for free convective flow of a nanofluid past a chemically reacting horizontal plate in a porous media. Freidoonimehr et al. [23] considered analytical modeling of three-dimensional squeezing nanofluid flow in a rotating channel on a lower stretching porous wall. Rashidi et al. [24] performed a study of nonlinear MHD tribological squeeze film at generalized magnetic Reynolds numbers using DTM. Also Rashidi et al. [25] also reported an analysis of entropy generation in an MHD flow over a rotating porous disk with variable physical properties. Freidoonimehr et al. [26] gave detailed information on predictor homotopy analysis method for nanofluid flow through expanding or contracting gaps with permeable walls.

Keeping in view the above studies, we study theoretically the buoyancy effects on chemically reactive magneto-nanofluid past a moving vertical plate. We have extended the work of Das and Jana [15] with the novelty of considering the porous medium, radiation, heat source and Soret effect. The water-based nanofluid containing nanoparticles of Alumina (Al_2O_3) is considered in the current study.

Nomenclature:

u^* velocity component along the x- direction [$m.s^{-1}$]

T^* temperature [K]

C^* concentration [g/ml]

μ_{nf} dynamic viscosity of the nanofluid [Pa.s]

ρ_{nf} density of the nanofluid [$kg.m^{-3}$]

σ_{nf} electrical conductivity of the nanofluid [$ohm^{-1}\ s^{-1}$]

k_{nf} thermal conductivity of the nanofluid [$W.m^{-1}.K^{-1}$]

g acceleration due to gravity [$m.s^{-2}$]

q_r radiative heat flux

q_0 heat source

$(\rho C_p)_{nf}$ heat capacitance of the nanofluid

β_{nf} thermal expansion coefficient [K^{-1}]

β^*_{nf} mass transfer coefficient [m/s]

t time [sec]

Kr chemical reaction parameter

ϕ solid volume fraction of the nanoparticles [m.g]

ρ_f density of the base fluid [kg.m^{-3}]

ρ_s density of the nanoparticles

σ_f electrical conductivity of the base fluid [ohm^{-1} s^{-1}]

σ_s electrical conductivity of the nanoparticles

μ_f viscosity of the base fluid [Pa.s]

$(\rho C_p)_f$ heat capacitance of the base fluid

$(\rho C_p)_s$ heat capacitance of the nanoparticles

D mass diffusion coefficient

D_1 thermal diffusion coefficient

k_f thermal conductivity of the base fluid [W.m^{-1}.K^{-1}]

k_s thermal conductivity of the nanoparticles

Superscript * Dimensional

2. FORMULATION OF THE PROBLLEM

We consider an unsteady free convective, heat and mass transfer flow of a magneto-nano and heat generating fluid past an infinite vertical porous flat plate which is moving with an impulsive motion in the presence of chemical reaction. The x^*-axis along the plate in the upward direction vertically and y^*-axis is taken perpendicular to it. A uniform transverse magnetic field of strength B_0 is applied perpendicular to the plate (parallel to the y^*-axis). The plate coincides with the plane $y^* = 0$ and the fluid flow being restricted to $y^* > 0$. At time $t^* = 0$, the plate is assumed to be at rest with the constant ambient temperature T^*_∞ and the concentration

C_∞^*. At time $t^* > 0$, the plate starts moving in its own plane with the velocity λu_0 in the vertical direction, where u_0 is constant and the temperature of the plate is raised or lowered to T_w^* and the level of concentration is also maintained at C_w^*. It is assumed that the pressure gradient is neglected in this analysis. It is also assumed that a radiative heat flux q_r is applied in the normal direction to the plate and mass flux caused by the temperature differences which is termed as thermal diffusion effect is considered. The fluid is a water based nanofluid containing nanoparticles of Alumina (Al_2O_3). It is further assumed that the base fluid and the suspended nanoparticles are in thermal equilibrium. The values related to thermo physical properties of the Al_2O_3-water nanofluid are given in Table 1. It is assumed that the induced magnetic field generated by the fluid flow is negligible in comparison with the applied one so that we assume the magnetic field to be $\vec{B} \equiv (0, 0, B_0)$. Based on the above assumptions and in the paper of Das and Jana [15], the momentum, energy and concentration equations can be expressed as

$$\rho_{nf}\frac{\partial u^*}{\partial t^*} = \mu_{nf}\frac{\partial^2 u^*}{\partial y^{*2}} + g(\rho\beta)_{nf}(T^* - T_\infty^*) + g(\rho\beta^*)_{nf}(C^* - C_\infty^*) - \sigma_{nf}B_0^2 u^* \tag{1}$$

$$(\rho C_p)_{nf}\frac{\partial T^*}{\partial t^*} = k_{nf}\frac{\partial^2 T^*}{\partial y^{*2}} - \frac{\partial q_r^*}{\partial y} \tag{2}$$

$$\frac{\partial C^*}{\partial t^*} = D\frac{\partial^2 C^*}{\partial y^{*2}} + D_1\frac{\partial^2 T^*}{\partial y^{*2}} - K_r'(C^* - C^*_\infty) \tag{3}$$

$$\left.\begin{aligned}
&\mu_{nf} = \frac{\mu_f}{(1-\phi)^{2.5}}, \quad \rho_{nf} = (1-\phi)\rho_f + \phi\rho_s,\\
&(\rho C_p)_{nf} = (1-\phi)(\rho C_p)_f + \phi(\rho C_p)_s,\\
&(\rho\beta)_{nf} = (1-\phi)(\rho\beta)_f + \phi(\rho\beta)_s,\\
&(\rho\beta^*)_{nf} = (1-\phi)(\rho\beta^*)_f + \phi(\rho\beta^*)_s,\\
&\sigma_{nf} = \sigma_f\left[1 + \frac{3(\sigma-1)\phi}{(\sigma+2)-(\sigma-1)\phi}\right], \; \sigma = \frac{\sigma_s}{\sigma_f},
\end{aligned}\right\} \tag{4}$$

The effective thermal conductivity of the nanofluid given by Hamilton and Crosser model followed by Kakac and Pramuanjaroenkij [1] is given by

$$k_{nf} = k_f\left[\frac{k_s + 2k_f - 2\phi(k_f - k_s)}{k_s + 2k_f + \phi(k_f - k_s)}\right] \tag{5}$$

In Eqs. (1) – (5), the subscripts nf, f and s denote the thermo physical properties of the nanofluid, base fluid and nanoparticles, respectively.

The initial and boundary conditions are

$$t^* = 0 : u^* = 0,\ T^* = T^*_\infty, C^* = C^*_\infty \text{ for all } y^* \geq 0,$$
$$t^* > 0 : u^* = \lambda u_0, T^* = T^*_w, C^* = C^*_w \text{ at } y^* = 0, \tag{6}$$
$$t^* > 0 : u^* \to 0,\ T^* \to T^*_\infty, C^* \to C^*_\infty \text{ as } y^* \to \infty$$

where λ indicates the direction of the moving plate with $\lambda = 0$ for the stationary plate, while $\lambda = \pm 1$ for the forth and back movement of the plate.

Table 1: Thermo physical properties of water and nanoparticles [15]

Physical properties	Water/base fluid	Al_2O_3(alumina)
ρ (kg/m^3)	997.1	3970
C_p (J/kg K)	4179	765
k (W/m K)	0.613	40
$\beta \times 10^5$ (K^{-1})	21	0.85
ϕ	0.0	0.15
σ (S/m)	5.5 x 10^{-6}	35 x10^6

For an optically thick fluid, we can adopt Rosseland approximation for radiative flux. The Rosseland approximation from Das and Jana [15] applies to optically thick media and gives the net radiation heat flux q_r by the expression

$$q_r^* = -\frac{4\sigma^*}{3k^*}\frac{\partial T^4}{\partial y} \tag{7}$$

where $\sigma^* (= 5.67\times10^{-8}\,\mathrm{W/m^2K^4})$ is the Stefan-Boltzmann constant and $k^*(\mathrm{m}^{-1})$ the Rosseland mean absorption coefficient. We assume that the temperature difference within the flow is sufficiently small such that the term T^4 may be expressed as a linear function of temperature. This is done by expanding T^4 in a Taylor series about a free stream temperature T_∞ as follows:

$$T^4 = T_\infty^4 + 3T_\infty^3(T - T_\infty) + 6T_\infty^2(T - T_\infty)^2 + \ldots\ldots \tag{8}$$

Neglecting higher-order terms in equation (8) beyond the first order in $(T - T_\infty)$, we get

$$T^4 \approx 4T_\infty^3 T - 3T_\infty^4 \tag{9}$$

Using (7) and (9), (2) becomes

$$\frac{\partial T^*}{\partial t^*} = \frac{1}{(\rho C_p)_{nf}}\left(k_{nf} + \frac{16\sigma^* T_\infty^3}{3k^*}\right)\frac{\partial^2 T^*}{\partial y^{*2}} + \frac{q_0}{(\rho C_p)_{nf}}(T^* - T^*_\infty) \tag{10}$$

We introduce the following non-dimensional variables

$$y = \frac{u_0 y^*}{\nu_f},\ t = \frac{u_0^2 t^*}{\nu_f},\ u = \frac{u^*}{u_0},\ \theta = \frac{T^* - T^*_\infty}{T^*_w - T^*_\infty},\ C = \frac{C^* - C^*_\infty}{C^*_w - C^*_\infty} \tag{11}$$

Eqs. (1), (3) and (10) reduces to the form

$$\frac{\partial u}{\partial t}=a_1\frac{\partial^2 u}{\partial y^2}+Gra_2\theta+Gca_5C-M^2a_3u \tag{12}$$

$$\frac{\partial \theta}{\partial t}=a_4\frac{\partial^2 \theta}{\partial y^2}+\frac{Du}{\Pr x_3}\frac{\partial^2 C}{\partial y^2} \tag{13}$$

$$\frac{\partial C}{\partial t}=\frac{1}{Sc}\frac{\partial^2 C}{\partial y^2}+So\frac{\partial^2 \theta}{\partial y^2}-KrC \tag{14}$$

where

$$a_1=\frac{1}{(1-\phi)^{2.5}x_1} \qquad a_2=\frac{x_2}{x_1},$$

$$a_3=\frac{x_5}{x_1} \qquad a_4=\frac{1}{x_3\Pr}(x_4+R)$$

$$x_1=\left[(1-\phi)+\phi\left(\frac{\rho_s}{\rho_f}\right)\right]$$

$$x_2=\left[(1-\phi)+\phi\left(\frac{(\rho\beta)_s}{(\rho\beta)_f}\right)\right] \qquad x_3=\left[(1-\phi)+\phi\left(\frac{(\rho C_p)_s}{(\rho C_p)_f}\right)\right]$$

$$x_4=\left[\frac{k_s+2k_f-2\phi(k_f-k_s)}{k_s+2k_f+\phi(k_f-k_s)}\right] \qquad x_5=\left[1+\frac{3(\sigma-1)\phi}{(\sigma+2)-(\sigma-1)\phi}\right]$$

$$x_6=\frac{x_4}{x_3}$$

$M^2=\dfrac{\sigma_f B_0^2\nu_f}{\rho_f u_0^2}$ (Magnetic parameter),

$R=\dfrac{16\sigma^* T_\infty^3}{3k_f k^*}$ (Radiation parameter),

$\Pr=\dfrac{\mu_f C_p}{k_f}$ (Prandtl number),

$$Gr = \frac{g\beta_f \mu_f (T_w^* - T_\infty^*)}{u_0^3} \quad \text{(Grashof number)},$$

$$Gc = \frac{g(\beta^*)_f \mu_f (C_w^* - C_\infty^*)}{u_0^3} \quad \text{(solutal Grashof number)},$$

$$Sc = \frac{\nu_f}{D} \quad \text{(Schmidt number)},$$

$$So = \frac{D_1}{\nu_f}\left(\frac{T_w^* - T_\infty^*}{C_w^* - C_\infty^*}\right) \quad \text{(Soret number)},$$

$$K = \frac{K_p^* u_0^2}{\nu_f^2} \quad \text{(Porosity parameter)},$$

$$Kr = \frac{K_r' \nu_f}{u_0^2} \quad \text{(chemical reaction parameter)}$$

$$Q = \frac{q_0 \nu_f^2}{k_f u_0^2} \quad \text{(Heat source parameter)}$$

The corresponding initial and boundary conditions are

$$\begin{aligned} &t = 0 : u = 0,\ \theta = 0,\ C = 0 \ \text{ for all } \ y \geq 0, \\ &t > 0 : u = \lambda,\ \ \theta = 1,\ \ C = 1 \quad \text{at } y = 0, \\ &t > 0 : u \to 0,\ \theta \to 0,\ C \to 0 \ \text{ as } \ y \to \infty \end{aligned} \tag{15}$$

3. SOLUTION OF THE PROBLEM

Equations (12) - (14) are linear partial differential equations and are to be solved with the initial and boundary conditions (15). For this set of equations the exact solution is not possible and hence we solve these equations by the finite-difference method. The equivalent finite difference schemes of equations (12) - (14) are as follows:

$$\begin{aligned} \frac{u_{i,j+1} - u_{i,j}}{\Delta t} = a_1 \frac{u_{i-1,j} - 2u_{i,j} + u_{i+1,j}}{(\Delta y)^2} + Gr\, a_2\, \theta_{i,j} + Gc\, a_5\, C_{i,j} \\ - M^2 u_{i,j} - \frac{1}{K} u_{i,j} \end{aligned} \tag{16}$$

$$\frac{\theta_{i,j+1} - \theta_{i,j}}{\Delta t} = a_4 \frac{\theta_{i-1,j} - 2\theta_{i,j} + \theta_{i+1,j}}{(\Delta y)^2} + \frac{1}{x_3 \Pr} Q\, \theta_{i,j} \tag{17}$$

$$\frac{C_{i,j+1} - C_{i,j}}{\Delta t} = \frac{1}{Sc} \frac{C_{i-1,j} - 2C_{i,j} + C_{i+1,j}}{(\Delta y)^2} + So \frac{\theta_{i-1,j} - 2\theta_{i,j} + \theta_{i+1,j}}{(\Delta y)^2} \tag{18}$$

Here, the suffix i refers to y and j to time. The mesh system is divided by taking $\Delta y = 0.1$. From the initial condition in (15), we have the following equivalent:

$$u(i,0) = 0,\ \theta(i,0) = 0, C(i,0) = 0 \text{ for all } i$$

The boundary conditions from (15) are expressed in finite-difference form as follows

$$u(0,j)=\lambda,\ \theta(0,j)=1,\ C(0,j)=1 \text{ for all } j$$
$$u(i_{\max},j)=0,\ \theta(i_{\max},j)=0,\ C(i_{\max},j)=0 \text{ for all } j$$

(Here i_{max} is taken as 200.)

The velocity at the end of time step viz., $u(i, j+1)(i=1,200)$ is computed from (12) in terms of velocity, temperature and concentration at points on the earlier time-step. After that $\theta\ (i, j+1)$ is computed from (13) and then $C\ (i, j+1)$ is computed from (14). The procedure is repeated until $t = 0.5$ (i.e. $j = 500$). During computation Δt is chosen as 0.001.

Skin-friction:

The skin-friction in non-dimensional form is given by the relation

$$\tau=-\left(\frac{du}{dy}\right)_{y=0},\text{where } \tau=\frac{\tau^{1}}{\rho U_0^2}$$

Rate of heat transfer:

The dimensionless rate of heat transfer in terms of Nusselt number is given by

$$Nu=-\left(\frac{d\theta}{dy}\right)_{y=0}$$

Rate of mass transfer:

The dimensionless rate of mass transfer in terms of Sherwood number is given by

$$Sh=-\left(\frac{dC}{dy}\right)_{y=0}$$

4. RESULTS AND DISCUSSION

The variations in velocity, temperature and concentration are observed with the help of graphs drawn by taking different values for various parameters. Also the changes in skin friction and Nusselt number are studied under the influence of related parameters.

The velocity profile for different nano fluids is shown in Figure 1. The velocity is less for copper-water nano fluid when compared to the influence of other nano fluids. Figure 2 reveals that the fluid velocity accelerates for increasing values of magnetic parameter. The momentum boundary layer thickness decreases for increasing values of M for the cases of stationary plate ($\lambda = 0$) as well as moving plate ($\lambda = \pm 1$). Figure 3 displays the effect of Schmidt number on fluid velocity. It physically relates to the comparative thickness of the hydrodynamic boundary layer and mass-transfer boundary layer. It is observed that the velocity field decreases when Schmidt number increases for the cases of stationary plate ($\lambda = 0$) as well as moving plate ($\lambda = \pm 1$). The influence of chemical reaction parameter leads to enhance the velocity which can be seen in Figure 4. Temperature profiles under the effect of Prandtl number and radiation parameter are displayed in Figure 5. The rising values of Prandtl number leads to improve the temperature. But a reverse trend is seen in the case of radiation parameter. Figure 6 displays temperature profiles under the effect of diffusion thermo and chemical reaction parameter. The impact of chemical reaction causes a fall in the temperature and the influence of Dufour effect leads to enhance the temperature of the fluid. Figure 7 exhibits that the impact of thermal diffusion causes an improvement in the concentration whereas an opposite trend is noticed in the case of Schmidt number. Figure 8 presents the concentration profiles under the effect of chemical reaction parameter and Dufour effect. The concentration grows with rising values of chemical reaction parameter and decreasing values of Dufour number.

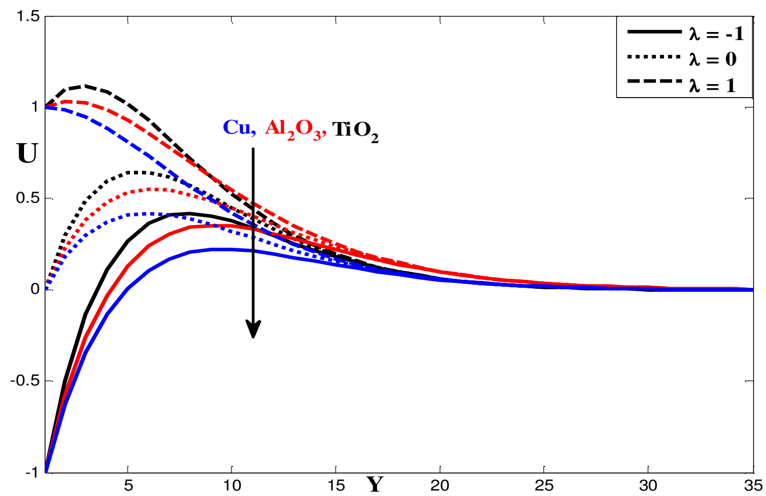

Figure 1: Velocity profiles for different nanofluids.

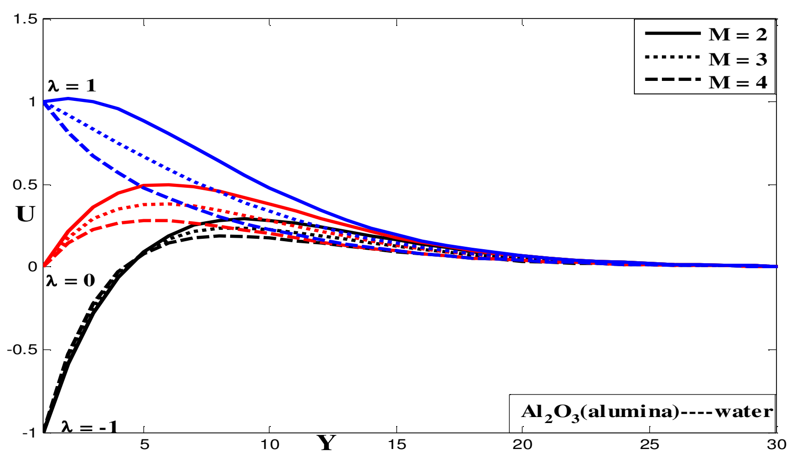

Figure 2: Velocity profiles under the effect of magnetic parameter.

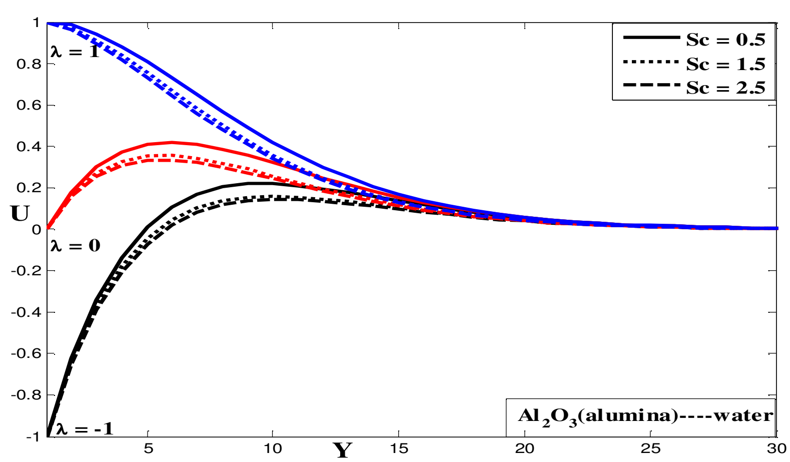

Figure 3: Velocity profiles under the effect of Schmidt parameter.

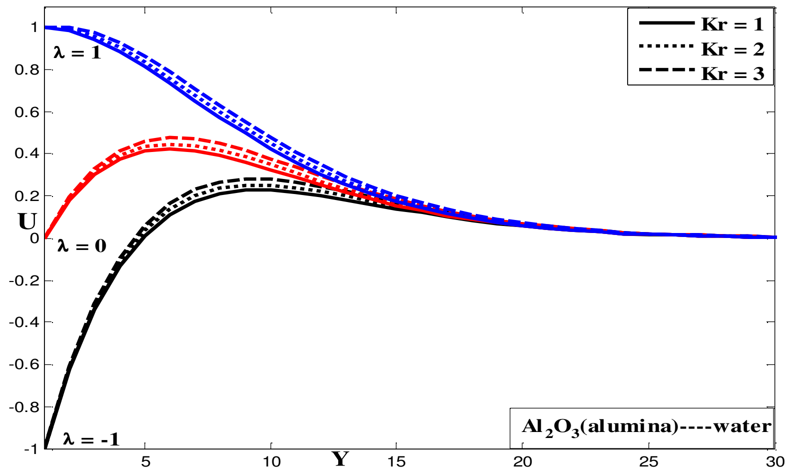

Figure 4: Velocity profiles under the effect of chemical reaction parameter.

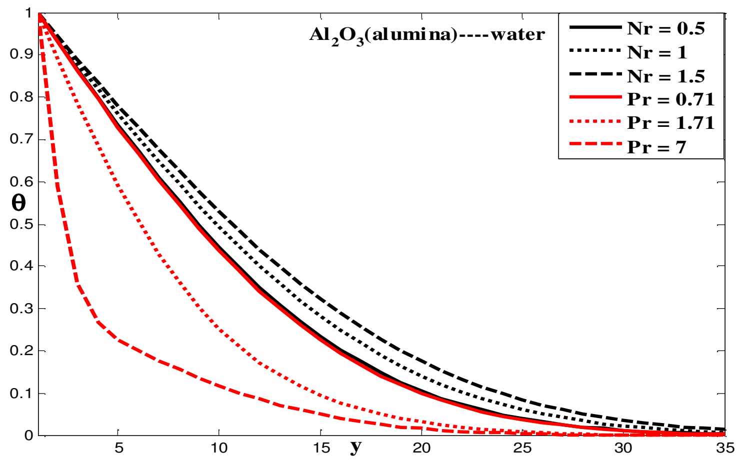

Figure 5: Temperature profiles under the effect of Prandtl number and radiation parameter.

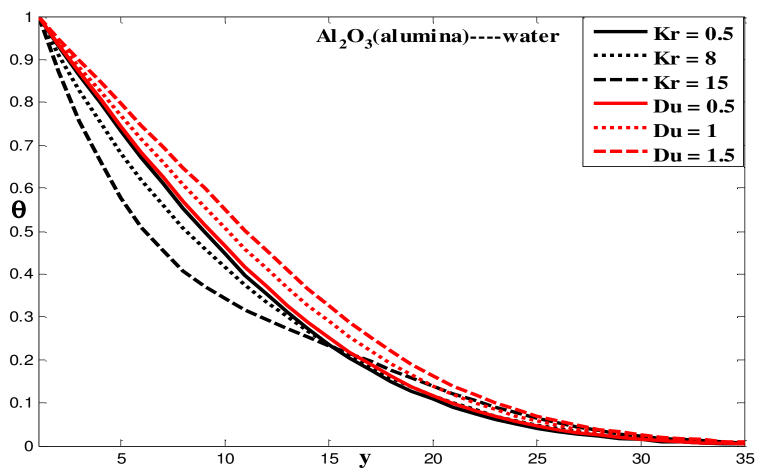

Figure 6: Temperature profiles under the effect of diffusion thermo and chemical reaction parameter.

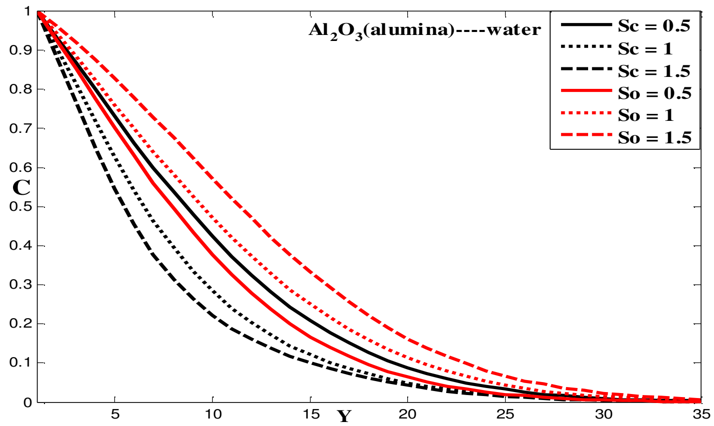

Figure 7: Concentration profiles under the effect of thermal diffusion and Schmidt parameter.

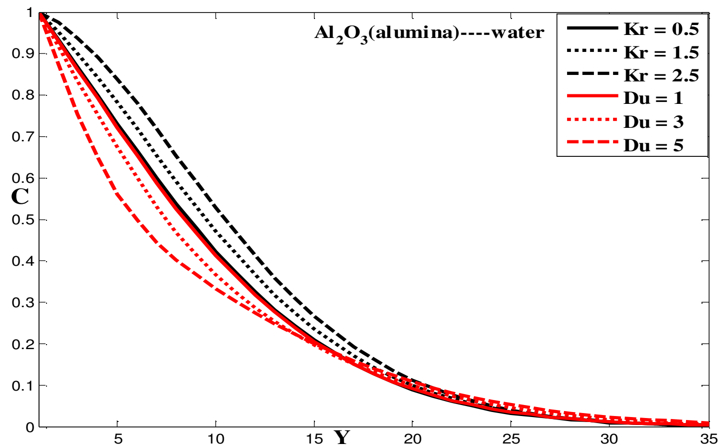

Figure 8: Concentration profiles under the effect of chemical reaction parameter and Dufour effect.

The variations in skin friction near the plate are presented in Figures 9-11. It can be noticed from Figure 9 that the impact of magnetic parameter leads to enhance the skin friction. Figure 10 shows that the skin friction comes down under the influence of chemical reaction parameter. Figure 11 displays skin friction variations under the influence of solid volume fraction. By increasing the volume of the nano particles an improvement in the skin friction is noticed. As the Prandtl number increases the rate of heat transfer increases. It is evident from Figure 12. Figure 13 displays the changes in Nusselt number under the influence of radiation, Schmidt parameter and thermal diffusion. For increasing values of radiation parameter and Schmidt number, the rate of heat transfer falls down, but a reverse effect is shown in the case of thermal diffusion.

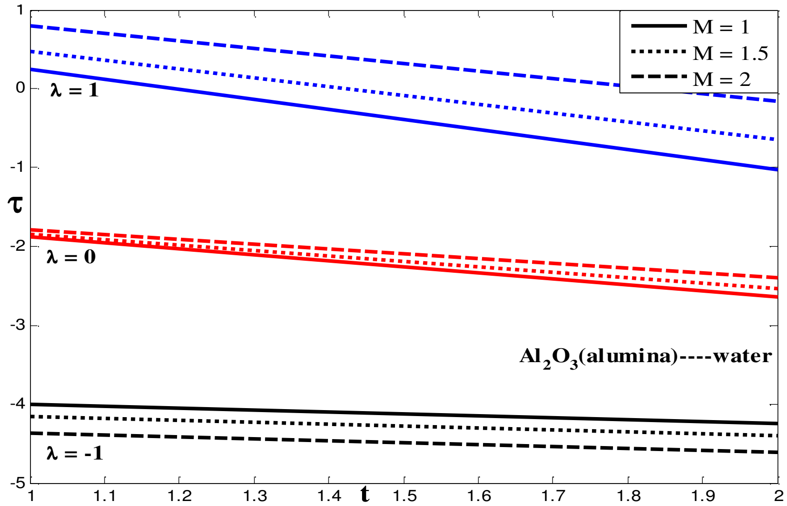

Figure 9: Skin friction under the influence of magnetic parameter.

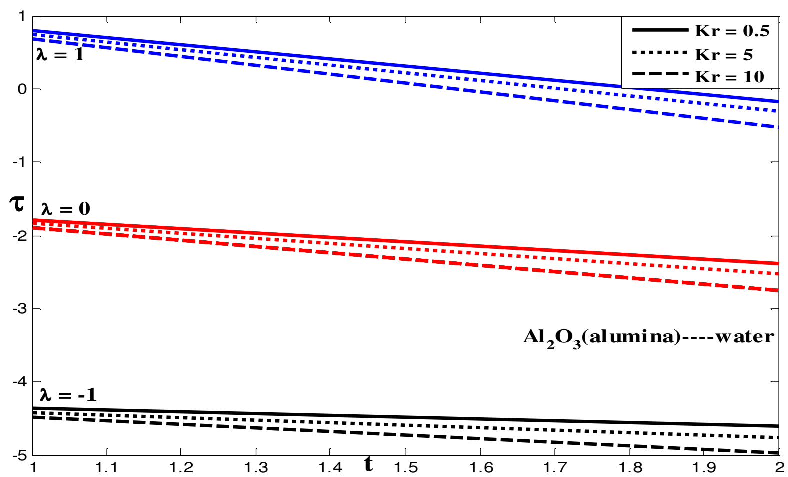

Figure 10: Skin friction under the influence of chemical reaction parameter.

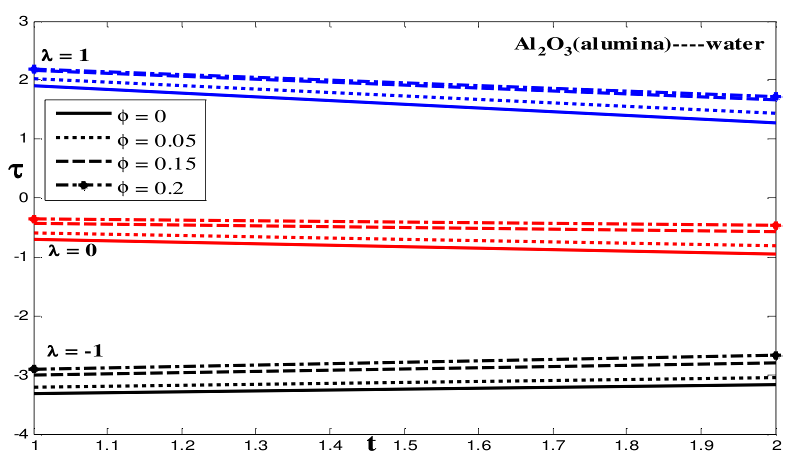

Figure 11: Skin friction under the influence of solid volume fraction.

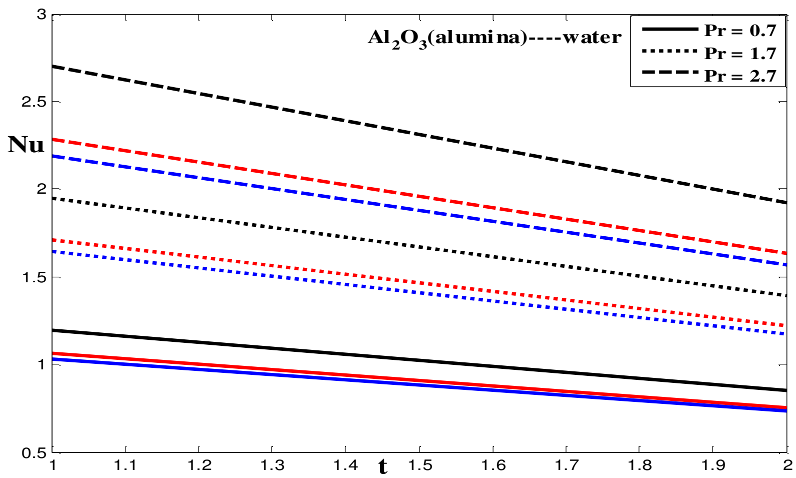

Figure 12: Nusselt number under the influence of Prandtl number.

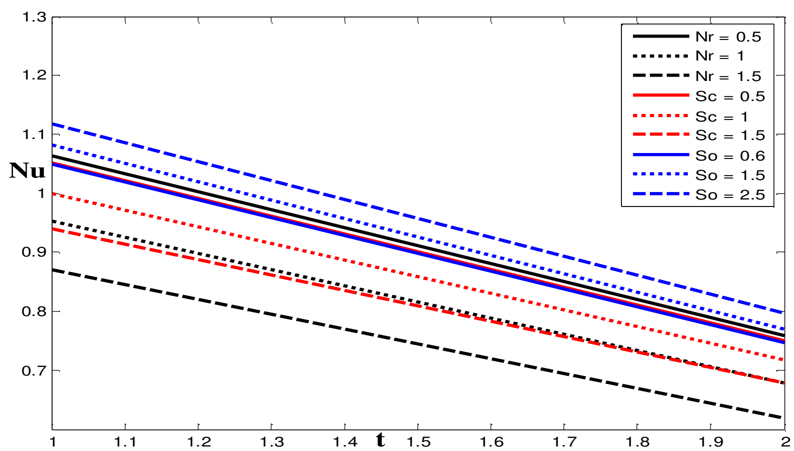

Figure 13: Nusselt number under the influence of radiation, Schmidt parameter and thermal diffusion.

5. CONCLUSIONS

The most interesting points of this study can be summarized as follows:

- The fluid velocity increases with increasing values of chemical reaction whereas opposite trend is shown in the case of magnetic parameter and Schmidt number.
- An increase in radiation parameter and Dufour number leads to enhance the fluid temperature. The rising values of Soret number and chemical reaction parameter serve to improve the species concentration.
- The increasing values of solid volume fraction enhance the shear stress at the plate but a reverse trend is noticed in the case of chemical reaction parameter.
- With an increase in radiation parameter and Schmidt parameter the rate of heat transfer decreases.

REFERENCES

[1] Kakac, S. and Pramuanjaroenkij, A. (2009). Review of convective heat transfer enhancement with nanofluids, *Int. Jour. Heat Mass Transfer*, 52, 3187–3196.

[2] Turkyilmazoglu, M. (2014). Exact analytical solutions for heat and mass transfer of MHD slip flow in nanofluids, *Chem. Eng. Sci.*, 84, 182–187.

[3] Srinivasacharya, D. and Upendar, M. (2013). Free convection in MHD micropolar fluid with Soret and Dufour effects, *Int. Jour. of Appl. Math. and Mech.*, 9 (5), 92-112.

[4] Raju, M.C., Varma, S.V.K., Reddy, P.V. and Saha, Sumon (2008). Soret effects due to natural convection between heated inclined plates with magnetic Field**,** *Jour. Mechanical Engineering*, ME39, 43-48.

[5] Chandra Reddy, P., Raju, M.C. and Raju, G.S.S. (2015). Thermal and solutal buoyancy effect on MHD boundary layer flow of a visco-elastic fluid past a porous plate with varying suction and heat source in the presence of thermal diffusion, *Journal of Applied & Computational Mathematics*, 4(5), 1-7.

[6] Makinde, O.D. and Aziz, A. (2010). MHD mixed convection from a vertical plate embedded in a porous medium with a convective boundary condition, *Int. Jour. Thermal Sciences*, 49, 1813-1820.

[7] Kandasamy, R., Wahib, B., Md. Raj and Khamis, Azme B. (2006). Effects of chemical reaction, heat and mass transfer on boundary layer flow over a porous wedge with heat radiation in presence of suction or injection, *Theoretical Applied Mechanics Belgrade*, 33(2), 123-148.

[8] Hayat, T., Abbasi, F.M., Al-Yami, M. and Monaquel, S. (2014). Slip and Joule heating effects in mixed convection peristaltic transport of nanofluid with Soret and Dufour effects, *Jou. Mol. Liq.*, 194, 93–99.

[9] Chandra Reddy, P., Raju, M.C. and Raju, G.S.S. (2016). Magnetohydrodynamic convective double diffusive laminar boundary layer flow past an accelerated vertical plate, *International Journal of Engineering Research in Africa*, 20 , 80-92.

[10] Chandra Reddy, P., Raju, M.C., Raju, G.S.S., Varma, S.V.K. (2016). Free convective magneto-nanofluid flow past a moving vertical plate in the presence of radiation and thermal diffusion, *Frontiers in Heat and Mass Transfer*, 7, 28 , 1-7.

[11] Chandra Reddy, P., Raju, M.C. and Raju, G.S.S. (2016). Free convective heat and mass transfer flow of heat generating nano fluid past a vertical moving porous plate in conducting field, *Special Topics and Reviews in Porous Media*, 7(2), 161-180.

[12] Chand, R. and Rana, G.C. (2015). Magneto convection in a layer of nanofluid in porous medium-A more realistic approach, *Journal of Nanofluids*, 4, 196-202.

[13] Anjali Devi, S.P. and Selvaraj, Mekala (2013). Thermal radiation effects of hydromagnetic flow of nanofluid over a nonlinearly stretching sheet in the existence of variable heat generation and viscous dissipation, *Int. Jour. Science and Research (IJSR)*, 4, 935-943.

[14] Murthy, P.V.S.N., Ram Reddy, C., Chamkha, A.J. and Rashad, A.M. (2014). Significance of viscous dissipation and chemical reaction on convective transport in a boundary layer stagnation point flow past a stretching / shrinking sheet in a nanofluid, *Jour. Nanofluids*, 4, 214-222.

[15] Das, S. and Jana, R.N. (2015). Natural convective magneto-nanofluid flow and radiative heat transfer past a moving vertical plate, *Alexandria Engg. Jour.*, 54, 55-64.

[16] Motsumi, T.G. and Makinde, O.D. (2012). Effects of thermal radiation and viscous dissipation on boundary layer flow of nanofluids over a permeable moving flat plate, *Physica Scripta*, 86, 4(045003), 1-8.

[17] Kameswaran, P.K., Narayana, M., Sibanda, P. and Murthy, P.V.S.N. (2012). Hydro-magnetic nanofluid flow due to a stretching or shrinking sheet with viscous dissipation and chemical reaction effects, *International Journal of Heat and Mass Transfer*, 55, 7587-7595.

[18] Nield, D.A. and Kuznetsov, A.V. (2011). The Cheng–Minkowycz problem for the double-diffusive natural convective boundary layer flow in a porous medium saturated by a nanofluid, *International Journal of Heat and Mass Transfer*, 54, 374-378.

[19] Ahmad, S., Rohni, A.M. and Pop, I. (2011). Blasius and Sakiadis problems in nanofluids, *Acta Mech.*, 218, 195-204.

[20] Abolbashari, M.H., Freidoonimehr, N., Nazari, F. and Rashidi, M.M. (2014). Entropy analysis for an unsteady MHD flow past a stretching permeable surface in nano-fluid, *Powder Technology*, 267, 256–267. doi.org/10.1016/j.powtec.2014.07.028

[21] Sheikholeslami, M. and Rashidi, M.M. (2015). Effect of space dependent magnetic field on free convection of Fe_3O_4 water nanofluid, *Journal of the Taiwan Institute of Chemical Engineers*, 56, 6–15.

[22] Rashidi, M.M., Momoniat, E., Ferdows, M. and Basiriparsa, A. (2014). Lie group solution for free convective flow of a nanofluid past a chemically reacting horizontal plate in a porous media, *Mathematical Problems in Engineering*, 2014, ID 239082, 21 pages.

[23] Freidoonimehr, N., Rostami, B., Rashidi, M.M. and Momoniat, E. (2014). Analytical modeling of three-dimensional squeezing nanofluid flow in a rotating channel on a lower stretching porous wall, *Mathematical Problems in Engineering*, ID 692728, 14 pages.

[24] Rashidi, M.M., Freidoonimehr, N., Momoniat, E. and Rostami, B. (2015). Study of nonlinear MHD tribological squeeze film at generalized magnetic Reynolds numbers using DTM, *PLoS ONE,* 10(8), 1-21.

[25] Rashidi, M.M., Mahmud, S., Freidoonimehr, N. and Rostami, B. (2015). Analysis of entropy generation in an MHD flow over a rotating porous disk with variable physical properties, *International Journal of Energy*, 16(4), 481–503.

[26] Freidoonimehr, N., Rostami, B. and Rashidi, M.M. (2015). Predictor homotopy analysis method for nanofluid flow through expanding or contracting gaps with permeable walls, *International Journal of Biomathematics*, 08, ID 1550050, 15 pages.